Quaternary Research 84 (2015) 82–95

Contents lists available at ScienceDirect

Quaternary Research

journal homepage: www.elsevier.com/locate/yqres

Age and sedimentary record of inland eolian sediments in Lithuania, NE European Sand Belt

Edyta Kalińska-Nartiša [a,b,*], Christine Thiel [c,d,e], Māris Nartišs [f], Jan-Pieter Buylaert [c,d], Andrew S. Murray [d]

[a] Department of Geology, Faculty of Science, Lund University, Sölvegatan 12, Lund S-223 62, Sweden
[b] Institute of Ecology and Earth Sciences, Department of Geology, Faculty of Science, University of Tartu, Ravila Str. 14A, Tartu EE50411, Estonia
[c] Centre for Nuclear Technologies (Nutech), Technical University of Denmark, Risø Campus, Frederiksborgvej 399, 4000 Roskilde, Denmark
[d] Nordic Laboratory for Luminescence Dating, Department of Geoscience, Aarhus University, Risø Campus, Frederiksborgvej 399, 4000 Roskilde, Denmark
[e] Leibniz Institute for Applied Geophysics, Section S3, Geochronology and Isotope Hydrology, Stilleweg 2, 30655 Hannover, Germany
[f] Faculty of Geography and Earth Sciences, University of Latvia, Alberta Str. 10, Riga LV1586, Latvia

ARTICLE INFO

Article history:
Received 5 August 2014
Available online 23 May 2015

Keywords:
Eolian deposits
Structural features
Textural features
Optically stimulated luminescence dating
European Sand Belt
Lithuania

ABSTRACT

We present a study based on four inland eolian locations in Eastern, Central and Southeastern Lithuania belonging to the northeastern part of the 'European Sand Belt' (ESB). Although there have been several previous studies of the ESB, this north-eastern extension has not been investigated before in any detail. The sedimentary structural–textural features are investigated and a chronology was derived using optically stimulated luminescence on both quartz and feldspar. The sedimentary structures and the rounding and surface characteristics of the quartz grains argue for a predominance of eolian transport. Additionally, some structural alternations and a significant contribution of non-eolian grains are interpreted as inherited local glacial/glaciofluvial-bearing lithologies.

Three main (glaciolacustrine–) eolian phases are distinguished based on the position in the landscape and the luminescence ages: (1) An *older eolian series* around 15 to 16 ka, possibly correlated with the cold GS-2a event according to the GRIP stratigraphy, and (2) a *younger eolian series* around 14.0 ka, possibly representing the GI-1d and 1c events. The *older eolian series* is underlain by (3) a *glaciolacustrine–eolian series* for which the period of deposition remains uncertain due to the significant discrepancy between the ages based on quartz and feldspar.

Introduction

Cold-climate eolian sediments are widespread in Europe; they make up a zone which is known as the 'European Sand Belt' (ESB) (Zeeberg, 1998; Koster, 2009), stretching from Great Britain, The Netherlands, Belgium, through Germany, to Poland, the Baltic States and to Russia. Its northwestern extent was first discussed by Van der Hammen (1951) and Van der Hammen and Wijmstra (1971). While these early studies concentrated on stratigraphical relationships, later work focused on establishing a chronological framework (Kasse, 1997; Bateman and Van Huissteden, 1999). Optically stimulated luminescence (OSL) dating is of importance in this context because it determines the time of deposition; one prerequisite for the application of this technique is the ideally full re-setting of the luminescence signal prior to sediment deposition (Wintle, 2008). This resetting occurs while the mineral grains of interest (quartz or feldspar) are exposed to sunlight, i.e., during transport and while exposed on surfaces. Eolian sediments in particular meet this important requirement, and are recognized as very suitable candidates for OSL dating. Based on OSL ages, different eolian phases within the ESB have been identified (Koster, 2005; Kolstrup, 2007; Vandenberghe et al., 2013) and this has made correlation possible for sediments within Western and Central Europe (e.g., Koster, 2005; Kasse et al., 2007; Tolksdorf and Kaiser, 2012). In addition, buried organic horizons are wide-spread in the inland dunes of Western and Central Europe; these important chronostratigraphic markers have been radiocarbon dated and used for correlations (Kaiser et al., 2009; Jankowski, 2012; Küster et al., 2014).

In contrast, chronological studies allowing detailed paleoenvironmental reconstruction of the northeastern part of the ESB are still rare. Most reconstructions of both inland and coastal eolian sequences from Lithuanian localities are based on indirect chronologies. Attempts have been made to radiocarbon date some sites; however, paleosols and other organic-rich material are found only rarely (Gudelis and Michaliukaitė, 1976; Gudelis, 1998; Gaigalas and Pazdur, 2008). Only one radiocarbon age from the inland eolian sediments in this region is available, from the Dzūkija dune massif in southern Lithuania (Blažauskas et al., 1998). At this site a yellowish-brown gyttja with mollusc remnants is located between the upper eolian fine-grained massive sequences and the lower horizontally bedded glaciofluvial sediments. On the basis of its 13.4 ± 0.14 cal ka BP age (Blažauskas et al., 1998) the gyttja has been associated with the Allerød Interstadial;

* Corresponding author at: Department of Geology, Faculty of Science, Lund University, Sölvegatan 12, Lund S-223 62, Sweden.
E-mail address: edyta.kalinska-nartisa@geol.lu.se (E. Kalińska-Nartiša).

http://dx.doi.org/10.1016/j.yqres.2015.04.001
0033-5894/

there seems to be a discontinuity between this formation and the underyling glaciofluvial material, and with the overlying fine-grained sands (possibly originating from the Atlantic period: Molodkov and Bitinas, 2006).

Other attempts have been made to date the eolian sediments directly using luminescence. Satkūnas et al. (1991) reported on the application of TL to a sedimentary succession from the Skersabaliai eolian massif between River Neris and River Vilnia. Their four TL ages increased with the depth and ranged from 13.2 to 10.0 ka; no errors were given. In later studies, Bitinas (2004) and Molodkov and Bitinas (2006) derived OSL ages using potassium- (K-) rich feldspar from three boreholes and one natural outcrop of three different large dune massifs in Lithuania. The ages of the eolian sequence found in the boreholes ranged from 5.0 ± 0.6 to 3.2 ± 0.5 ka (Dzūkija borehole), 10.6 ± 1.5 to 4.4 ± 1.0 ka (Viduklė borehole) and 8.4 ± 2.3 to 5.9 ± 0.5 ka (Žalioji Giria borehole), respectively. For the natural outcrop in Dzūkija, they derived ages of between 6.2 ± 3.1 and 5.9 ± 0.6 ka. The glaciolacustrine sediments directly underlying the eolian sequence were dated to between 8.2 ± 0.6 and 7.5 ± 1.7 ka (Dzūkija borehole) and 11.3 ± 1.4 ka (Žalioji Giria borehole). Based on these data, it appears that eolian activity started after the drainage of the lacustrine basins during the Younger Dryas and Preboreal periods. These results provided a chronological foundation for their study of the Late Glacial and Holocene sedimentary history in the region, and they distinguished between sediments from the Younger Dryas, the Preboreal, the end of the Atlantic period, and (in some localities) the Subboreal.

In addition to these studies making use of direct and indirect ages, there is information on the local ice margin of the Last Glacial Maximum (LGM), together with numerous lithological and paleobotanical investigations (Stančikaitė et al., 2004, 2009; Stančikaitė, 2006; Satkūnas et al., 2009). However, in this part of the ESB there are very few studies which bring numerical ages together with information on sedimentological (structural–textural features) and stratigraphic characteristics (Satkūnas et al., 1991; Molodkov and Bitinas, 2006; Kalińska-Nartiša et al., 2014).

Here we report on a new detailed study of inland dunes at four locations: Mikieriai, Inkliuzai, Gaižiūnai and Rūdninkai (Fig. 1). The existence of fresh outcrops and the lack of previous research make them ideal for a structural–textural investigation and numerical age determination. Quartz is abundant in these sediments; because of its mechanical and chemical resistance, the analysis of its shape and the surface character, as well as the proportion of other types of minerals within the sediments give information on paleoenvironmental conditions (Vieira et al., 2003; Darrénougué et al., 2009; Velichko et al., 2009; Woronko, 2012; Kalińska and Nartišs, 2014). In addition, associated processes such as weathering, corrasion and deflation (Akulov and

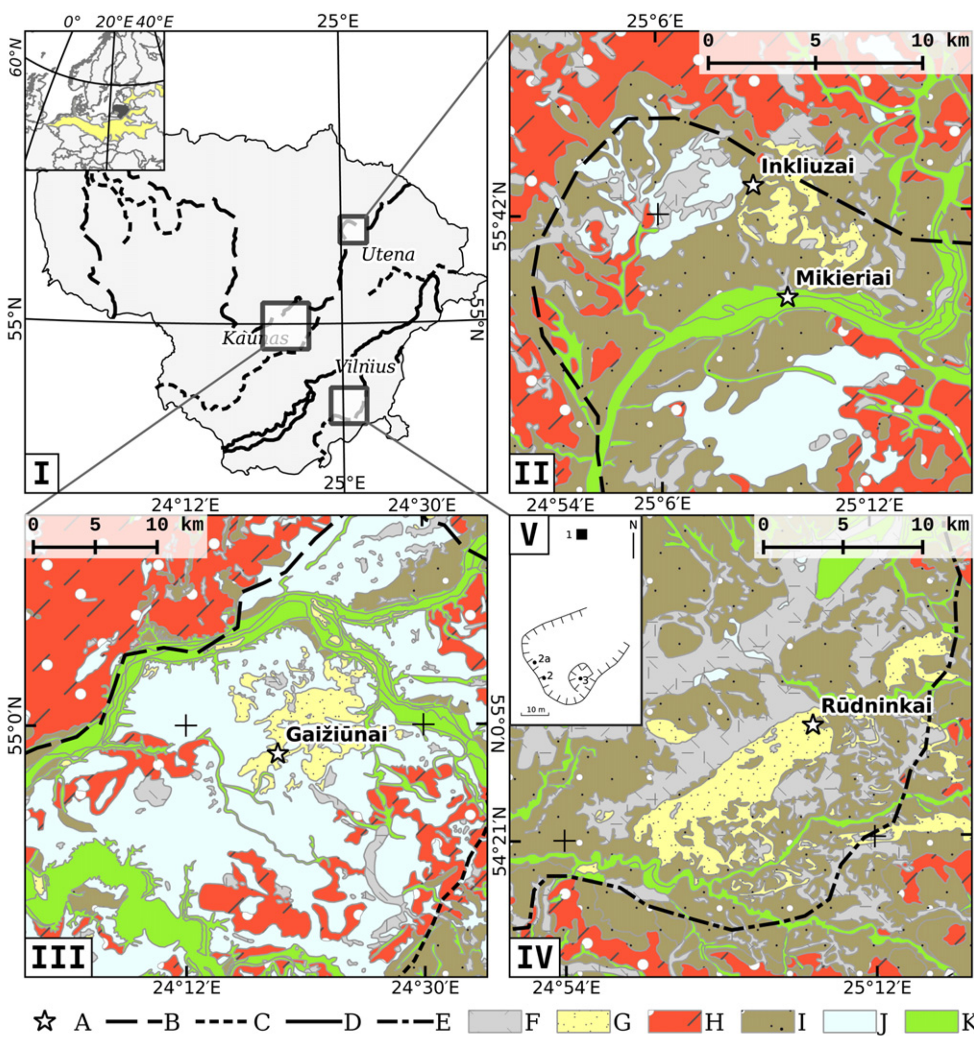

Figure 1. Site location in Lithuania (I). Detailed geological situation: II = Inkliuzai and Mikieriai. III = Gaižiūnai. IV = Rūdninkai. Profiles location at Rūdninkai site (V). Legend: A = sites. B–E = Ice-margin limits (according to Guobytė and Satkūnas, 2011). B: Middle Lithuania. C: South Lithuania. D: Baltija. E: the Last Glacial Maximum (LGM). F–K = Quaternary sediments. F = Peats. G = Eolian sands. H = Glacial sediments. I = Glaciofluvial sands and gravels. J = Glaciolacustrine sands. K = Fluvial sands.

https://doi.org/10.1016/j.yqres.2015.04.001 Published online by Cambridge University Press

Rubtsova, 2011; Woronko and Hoch, 2011), and the source and maturity of the deposits (Muhs, 2004; Kasper-Zubillaga and Zolezzi-Ruiz, 2007) are investigated. An OSL chronology for these deposits is constructed, based on both quartz and feldspar in order to provide robust age information and check the completeness of bleaching of the quartz OSL signal (cf. Murray et al., 2012); such a comparison has never been undertaken for the northeastern ESB sediments. Our multidisciplinary approach allows the reconstruction of depositional history, variability and overall patterns within the sedimentary environment during the Late Glacial period.

Geological setting and existing chronological data

Four eolian sediment sequences (Fig. 1) representing northeastern, central and southeastern Lithuania within the north-eastern part of the ESB (Zeeberg, 1998) were chosen for these investigations: Inkliuzai and Mikieriai (northeastern Lithuania), Gaižiūnai (central Lithuania), and Rūdninkai (southeastern Lithuania). These sites are representative of the largest units of continental dunes in the region (cf. Molodkov and Bitinas, 2006); all are located within the limits of the ice extent of the LGM.

Inkliuzai and Mikieriai

Inkliuzai and Mikieriai are situated approximately 25 km NW of the town of Utena (Fig. 1.I) within a small dune field. The Inkliuzai site represents the NE-most edge of this dune field; Mikieriai, located on the right bank of River Šventoji, represents the southernmost end (Fig. 1.II). The Middle Lithuanian ice-marginal zone edge is located between approximately 1.5 and 5 km north of our sites; both glaciofluvial and glaciolacustrine sediments are found in the immediate surroundings. The eolian sediments of the Mikieriai site overlie fluvial sands of the higher terrace of the River Šventoji. The ^{10}Be age of the Middle Lithuanian ice-marginal zone is 13.5 $\pm$ 0.6 ka (Rinterknecht et al., 2006, 2008); this is in good agreement with the radiocarbon age of 13.6 $\pm$ 0.2 cal ka BP derived from organic matter recovered directly from above the uppermost till associated with this ice margin (Bitinas et al., 2002).

Most of the 1.9 m sedimentary successions of the Mikieriai site (Fig. 2A) consists of sand with climbing ripple cross-lamination (*Src*) in the sedimentary code proposed by Miall (1977, 1978); this changes to massive sand (*Sm*) in the upper part of the section. For sedimentary and mineralogical analyses samples were taken at 10–20 cm intervals. In addition, we collected one luminescence sample from the uppermost

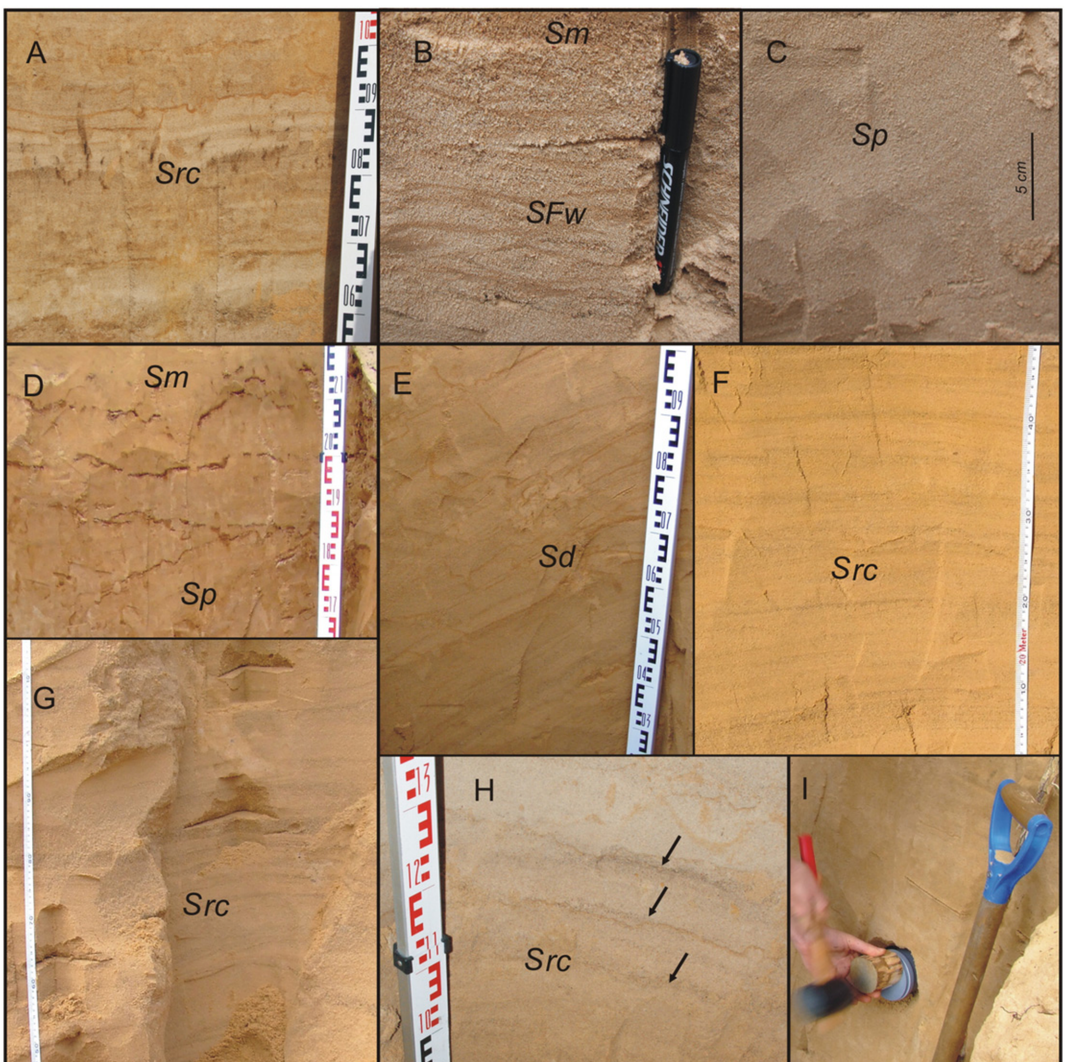

Figure 2. Typical sedimentary facies. A. climbing ripple cross-laminated (*Src*) sand; Mikieriai profile. B. wavy (*Sw*, *SFw*) and massive (*Sm*, *Fm*) sand; Inkliuzai profile. C. high-angle tabular cross-stratification (*Sp*); Inkliuzai profile. D. Contact between the high (planar) cross-stratified sand (*Sp*) and massive sand (*Sm*); Gaižiūnai site. E. High (planar) cross-stratified sand (*Sp*) with some deformations (*Sd*); Gaižiūnai site. F. climbing ripple cross-laminated (*Src*) sand; Rūdninkai 3 profile. G. climbing ripple cross-laminated (*Src*) sand; Rūdninkai 2 profile. H. climbing ripple cross-laminated (*Src*) sand with alternating coarser and finer sand (marked by arrows); Rūdninkai 1 profile. G. Luminescence sampling.

https://doi.org/10.1016/j.yqres.2015.04.001 Published online by Cambridge University Press

(*Sm*) section of the profile. Some wavy (*SFw*) and massive (*Sm*) structure (Fig. 2B) alternations can be observed in the 1.4 m Inkliuzai profile. In contrast to Mikieriai, the lowermost part of the Inkliuzai profile consists of high-angle tabular cross-stratification (*Sp*) (Fig. 2C). Samples were taken only from the sandy horizons in the profile, and one luminescence sample was taken from the uppermost (presumed eolian) part.

Gaižiūnai

The Gaižiūnai site is taken to represent the southwestern part of the large dune field of Central Lithuania. It is situated close to the city of Kaunas (Fig. 1.I) and the River Neris. Dunes formed on the surface of the broad glaciolacustrine plain (Fig. 1.III) located outside of the Middle Lithuanian ice-marginal zone, but within the Southern Lithuanian zone (Guobytė and Satkūnas, 2011). The age of the latter ice-marginal zone is thought to be between 14.6 and 12.0 ka based on ^{10}Be exposure ages (Rinterknecht et al., 2006, 2008); these ages do not allow clear differentiation between the Middle Lithuanian and Southern Lithuanian ice-marginal zone. Sands with both planar cross-stratification (*Sp*) and massive structure (*Sm*) are present in the 2.6 m Gaižiūnai profile (Fig. 2D). The dipping angles vary between 15° and 37° to the east, and some deformations (*Sd*) and erosional surfaces can be observed (Fig. 2E). Samples were taken at 5–25 cm intervals (Fig. 3). Luminescence samples were taken from the middle and bottom part of the profile.

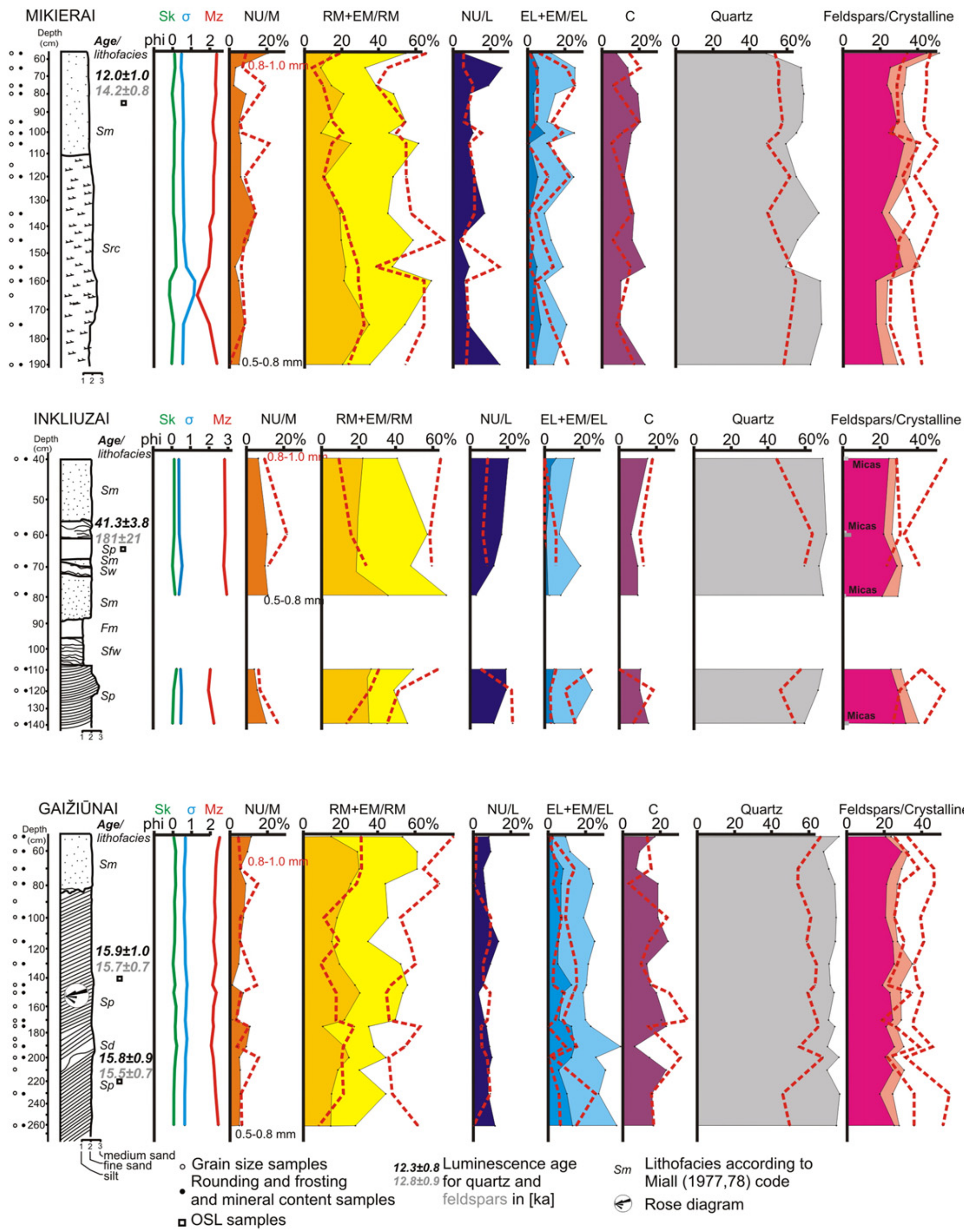

Figure 3. Sediment logs of Mikieriai, Inkliuzai, and Gaižiūnai showing the results of textural feature analysis. Sk = skewness. σ = standard deviation. Mz = mean. NU/M = non-abraded matt quartz grains. RM = well-rounded matt. EM/RM = partially-rounded matt. NU/L = non-abraded shiny. EL = well-rounded shiny. C = broken.

https://doi.org/10.1016/j.yqres.2015.04.001 Published online by Cambridge University Press

Rūdninkai

The Rūdninkai site is located approximately 35 km SSW of the city of Vilnius (Fig. 1.I), in the foreland of the Baltija ice-marginal zone ^{10}Be dated to 14.0 ± 0.4 ka (Rinterknecht et al., 2006, 2008). The site is located several km within the maximal extent of the Weichselian (Vistulian) glaciation, which according to Satkūnas (1993) reached its maximum extent no earlier than 22–21 ka, and began to retreat at 18.3 ± 0.8 ka (Rinterknecht et al., 2008). A prominent dune field stretches NW–SE for approximately 25 km, and is cut by the River Merkys next to the village of Rūdninkai (Fig. 1.IV). The eolian sediments are bordered by glaciofluvial and glaciolacustrine formations, representing the proximal part of an outwash-plain of a side-channel bar (Blažauskas et al., 2007) and the Vokė–Merkys–Nemunas drainage paleovalley which has been correlated with the retreating Baltija (Pomeranian) ice-margin (Guobytė and Satkūnas, 2011).

At Rūdninkai four profiles were investigated (Fig. 1.V): two (Rūdninkai 2 and 2a) in the uppermost part of the dune (Rūdninkai 3) and interdune (Rūdninkai 1); samples were taken every 10–30 cm for sedimentary analyses (Fig. 4). Yellowish sand with ripple cross-lamination (*Src*) can be found in all profiles (Figs. 2F, G, and H). The laminas dip at angles of 3–13° and 1–10° (Rūdninkai 2 and 2a, respectively) to the south-east. The uppermost part of the Rūdninkai 3 profile contains massive sand (*Sm*). Luminescence samples were taken from both

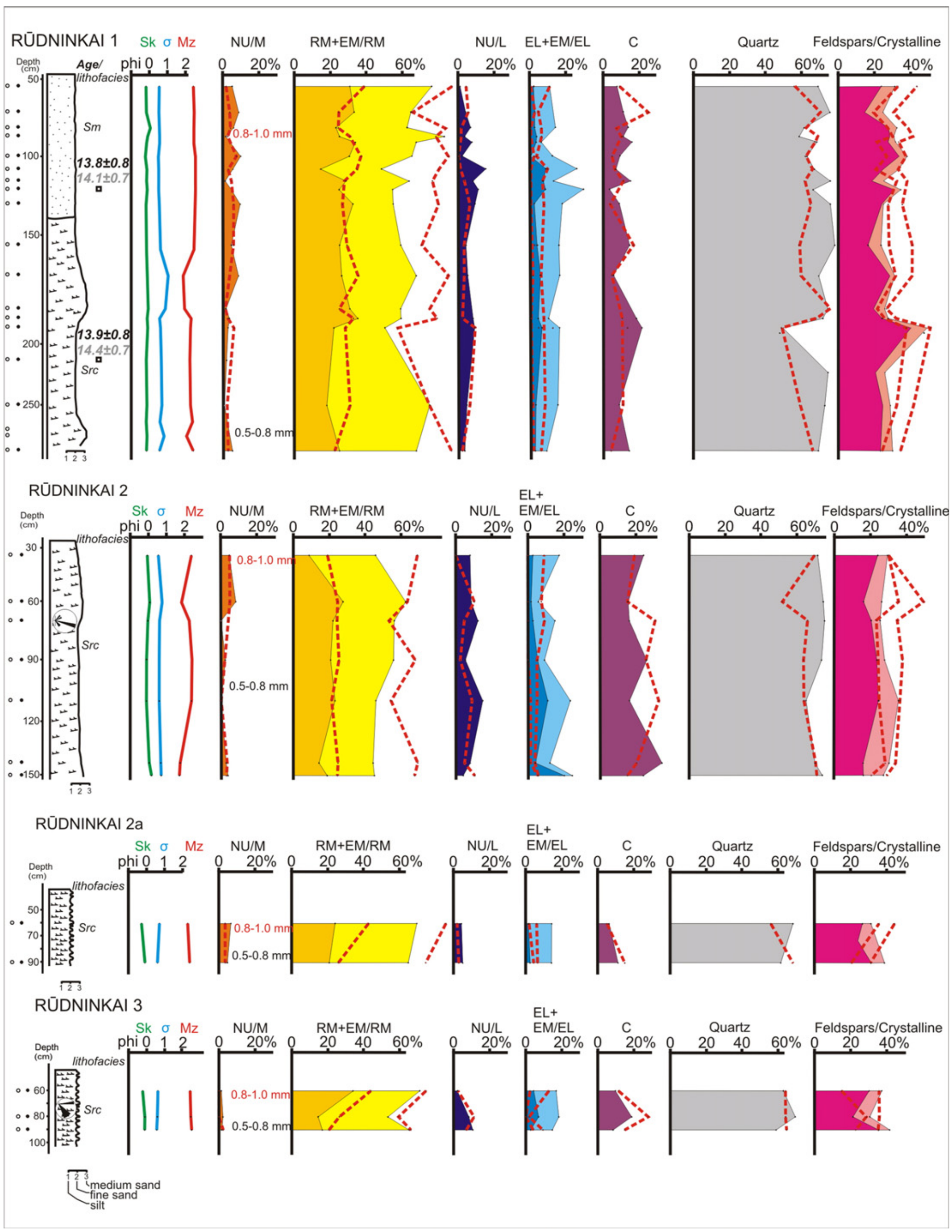

Figure 4. Sediment logs of Rūdninkai 1, 2, 2a and 3 profiles showing the results of textural feature analysis. For key see Fig. 3.

https://doi.org/10.1016/j.yqres.2015.04.001 Published online by Cambridge University Press

the massive and the ripple-cross sand within the Rūdninkai 3 profile (Fig. 2I).

Material and methods

In total, seven profiles were investigated: Gaižiūnai (one profile), Inkliuzai (one profile), Mikieriai (one profile) and Rūdninkai (four profiles). Our multidisciplinary sedimentological analyses included (1) grain-size distribution measurements, (2) investigations of rounding of the quartz grains and characterisation of the surface of the quartz grains in the sandy fractions, and (3) determination of the mineral–petrographic composition of the sandy fractions. In addition, the sediments were OSL dated using both coarse-grained quartz and K-rich feldspar. All these investigations are described below.

Sedimentological analyses

Grain-size analyses of 72 samples were performed by dry sieving. Based on the grain-size distributions it was possible to determine the logarithmic Folk and Ward (1957) graphical measures; the analyses for these values were conducted using the customised version of the R package 'rysgran' (Gilbert et al., 2012). The reconstruction of paleocurrent directions is based on the orientation of the cross-stratification, and presented as rose diagrams for the three profiles Gaižiūnai, Rūdninkai 2 and 2a (Figs. 3 and 4).

Two sandy fractions (0.5–0.8 and 0.8–1.0 mm) were used for classification of quartz grain shape and surface character using Cailleux (1942) with modifications of Mycielska-Dowgiałło and Woronko (1998). The samples were pre-treated as follows: (1) dry-sieving to obtain the appropriate fractions, (2) rinsing (approx. six times) with distilled water to remove smaller particles, especially clay, and (3) drying. To determine the rounding and frosting (matt) of the surfaces of the quartz grains a binocular microscope with 30–50× magnification was used. About 120–150 quartz grains were randomly selected from two sandy fractions, and then classified to one of the seven groups: (1) well-rounded matt (RM), (2) well-rounded shiny (EL), (3) partially rounded matt (EM/RM), (4) partially rounded shiny (EM/EL), (5) non-abraded matt (NU/M), (6) non-abraded shiny (NU/L), and (7) broken with at least 30% of the original grain surface (C). Each group of grains refers to a specific environment (Woronko, 2012): eolian and moderately eolian is represented by RM and EM/RM, respectively; high-energy and moderately high-energy aquatic EL and EM/EL, respectively; with no signs of rounding during transport nor evidence of any post-depositional weathering (NU/L); 'in situ' weathered, not affected by transport (NU/M); and cracking conditions (C) resulting from an active layer under repetitive cycles of freezing and thawing during cold periods of the Pleistocene. Analysis of the 0.5–0.8 and 0.8–1.0 mm fraction was performed on 66 and 62 samples, respectively (Gaižiūnai: 16 (14) samples for the 0.5–0.8 (0.8–1.0) mm fraction; Inkliuzai: 7 (6), Mikieriai: 14 (13), Rūdninkai: 29 (29)).

In addition, the mineral–petrographic composition was determined from both the 0.5–0.8 and the 0.8–1.0 mm fraction to check for redeposition. It is known that the amount of quartz increases with reworking/redeposition (Mycielska-Dowgiałło, 2007). 200–250 grains were randomly chosen and four mineral groups were distinguished (in %): quartz, feldspars, particles of crystalline rocks, and micaceous minerals.

Optically stimulated luminescence dating

Six samples from four profiles (two each for Gaižiūnai and Rūdninkai, and one each for the other two sites) were collected for luminescence dating. The samples were collected in 0.5 m long opaque PCV tubes that were hammered into the freshly cleaned surface of the pits (cf. Fig. 2I). The tubes were dug out and sealed promptly to prevent further light exposure.

The samples were opened and further treated under subdued orange light. The light-exposed material at each end of the tube was reserved for dose rate determination; only the material from the inner part of the tube was prepared for D_e measurement. The 180–250 μm fraction was extracted following standard laboratory procedures, i.e., wet sieving, 10% hydrochloric acid (HCl) for 1 h to remove carbonates, 10% hydrogen peroxide (H_2O_2) for 1 h to remove organic material, 10% hydrofluoric acid (HF) to clean the outer surface of the grains and to remove the external alpha contribution to feldspar grains, and heavy liquid separation ($\rho = 2.58\ g\cdot cm^{-3}$) to separate quartz from K-rich feldspar. The quartz-rich extract ($\rho > 2.58\ g\cdot cm^{-3}$) was subsequently etched with 40% HF for 1 h to remove any remaining feldspar and the outer alpha-irradiated layer. After etching, the quartz extracts were treated with 10% HCl for 1 h to remove any soluble fluorides which might have build-up during HF treatment. Subsequently, the samples (both quartz and K-feldspar fractions) were re-sieved to ensure no grains <180 μm were present.

The portions for dose-rate determination were dried, ignited (24 h at 450°C), mechanically ground and thus homogenised, and cast in wax in a defined geometry. Prior to radionuclide concentration measurements using a high-resolution gamma spectrometer (Murray et al., 1987) the casts were stored for at least three weeks to ensure equilibrium between radon and its daughter nuclides. The measured radionuclide concentrations were converted into beta and gamma dose rates following Olley et al. (1996). The calculation of the contribution of the cosmic dose rate is based on Prescott and Hutton (1994). For the K-rich feldspar extracts, an internal beta dose rate was calculated based on a K content of 12.5 ± 0.5% (Huntley and Baril, 1997) and a Rb content of 400 ± 100 ppm (Huntley and Hancock, 2001). The dependence of beta dose-rate attenuation on grain-size was based on Mejdahl (1979). An effective internal alpha dose-rate contribution from U and Th of 0.06 ± 0.03 Gy/ka was included for both quartz and K-feldspar. A life-time average burial water content of 9 ± 4% was assumed for all samples; this value is based on field observations, and the uncertainty takes into account inevitable fluctuations in water content with time. The resulting total dose rates are listed in Table 1. Note that the ^{238}U concentrations are not sufficiently well-known to discuss disequilibrium in the U-series on a sample by sample basis. However, the average $^{226}Ra/^{238}U$ activity concentration ratio is 1.02 ± 0.09 indicating that on average the first part of the U-series was probably close to equilibrium during burial.

All luminescence measurements were undertaken on automated Risø TL/OSL readers (model DA-20) equipped with calibrated $^{90}Sr/^{90}Y$ beta sources. For quartz, blue-light emitting diodes (LEDs) were used for stimulation, and the luminescence was detected through a Hoya U-340 ultraviolet filter, while for the K-rich feldspar extract infrared (IR) diodes and a blue filter package (Schott BG39/Corning 7–59 filters) were used.

The purity of the quartz was checked following Duller (2003). Tests on three aliquots per sample showed that all samples were sufficiently pure (OSL IR depletion ratio within 1.0 ± 0.1). From these measurements it was further evident that the OSL signal in this quartz is dominated by the fast component, a prerequisite for reliable quartz OSL dating. For D_e measurements a single aliquot regenerative dose protocol (SAR; Murray and Wintle, 2000) was applied, with a preheat of 260°C (10 s) and blue stimulation at 125°C (100 s). The response to a test dose of ~5 Gy was measured in the same way after preheating to 220°C (0 s). A high-temperature clean-out (blue light) was employed at the end of each SAR cycle to minimise any signal carry-over. The initial 0.4 s of the decay curve less a background of the subsequent ~2 s were used to construct the growth curves which were fitted with a single exponential function. All aliquots passed the standard quality control criteria (e.g., Wintle and Murray, 2006).

Table 1
Summary of radionuclide concentrations, total dose rates (D_r), equivalent doses (D_e) and ages for both quartz (OSL) and K-feldspar ($pIRIR_{290}$). A water content of 9 ± 4% was used for all samples based on field observations. n = number of aliquots measured to obtain average D_e's. Uncertainties are given as standard errors.

Field ID	Lab code	^{238}U (Bq/kg)	^{226}Ra (Bq/kg)	^{232}Th (Bq/kg)	^{40}K (Bq/kg)	Dose rate quartz (Gy/ka)	Dose rate K-feldspar (Gy/ka)	n for OSL	OSL De (Gy)	n for $pIRIR_{290}$	$pIRIR_{290}$ De (Gy)	OSL age (ka)	$pIRIR_{290}$ age (ka)
Gaiziunai 0,5 (XXVII)	123097	14 ± 5	11.6 ± 0.4	13.7 ± 0.5	353 ± 9	1.61 ± 0.07	2.44 ± 0.08	16	25.4 ± 0.5	6	38.4 ± 0.9	15.8 ± 0.9	15.7 ± 0.7
Gaiziunai 1,3 (XXIX)	123099	17 ± 6	13.0 ± 0.5	16.7 ± 0.6	331 ± 9	1.65 ± 0.08	2.47 ± 0.09	8	26.2 ± 1.1	6	38.3 ± 0.7	15.9 ± 1.0	15.5 ± 0.7
Inkluzai 0,75 (XXV)	123095	16 ± 7	16.1 ± 1.3	16.4 ± 0.6	534 ± 13	2.28 ± 0.10	3.10 ± 0.11	13	93 ± 8	6	560 ± 60	41 ± 4	180 ± 20
Mikieriai 2,1 (XXVI)	123096	6 ± 5	7.0 ± 0.4	8.1 ± 0.4	357 ± 9	1.47 ± 0.07	2.29 ± 0.08	10	18.9 ± 1.1	6	33.5 ± 1.3	12.9 ± 1.0	14.2 ± 0.8
Rudninkai 0,9 (XXVIII)	123098	6 ± 4	8.5 ± 0.3	10.4 ± 0.3	352 ± 9	1.50 ± 0.07	2.32 ± 0.08	14	20.9 ± 0.5	6	32.7 ± 0.8	13.9 ± 0.8	14.1 ± 0.7
Rudninkai 1,7 (XXX)	H23001	7 ± 4	6.7 ± 0.3	8.0 ± 0.3	336 ± 9	1.41 ± 0.06	2.24 ± 0.08	11	19.5 ± 0.5	6	32.2 ± 0.8	13.8 ± 0.8	14.4 ± 0.7

To test whether the measurement protocol can accurately measure a dose given prior to heating (the conditions in nature) a dose recovery test was conducted on all samples. Three aliquots were each stimulated (bleached) using blue LED exposure for 100 s. After a pause of 10 ks the aliquots were again bleached to ensure that there was minimal thermally transferred OSL signal in the sample. Subsequently a dose similar to the natural dose was given to each aliquot, and these were then measured using the standard SAR protocol described above. The average measured to given dose ratio was 0.90 ± 0.05 (n = 18); this implies that our measurement protocol is able to measure accurately a dose given before any thermal pre-treatment (Wintle and Murray, 2006).

The K-rich feldspar extracts were measured following Thiel et al. (2011). The reliability of this approach has been shown by Buylaert et al. (2012). After a preheat of 320°C and an IR bleach at 50°C for 200 s (IR_{50}), the post-IR IRSL was measured at an elevated temperature (200 s at 290°C; $pIRIR_{290}$). A test dose of about 10 Gy was administered prior to measuring the test dose IRSL response in the same manner as the natural and regenerative doses. At the end of each measurement cycle an IR illumination at 325°C (100 s) was inserted. The growth curves were fitted with a single exponential function using the initial 1.5 s of the decay curve, minus a background of the last 40 s. For all aliquots, recycling (repeated regenerative dose measurement) was within 5%, and recuperation (signal after administering zero dose) was well below 5%.

The applicability of this measurement protocol was also tested by means of a dose recovery test. Six aliquots each of sample Rūdninkai 0.9 (XXVIII) (laboratory ID 123098; cf. Table 1) and sample Gaižiūnai 1.3 (XXIX) (laboratory ID 123099) were bleached in a Hönle SOL 2 solar simulator for 4 h. Prior to measurements a dose close to the natural dose was then administered to three of the bleached aliquots per sample. The other three aliquots per sample were used to measure the residual signal after bleaching using the $pIRIR_{290}$ protocol described above. This residual (on average ~14 Gy) was subtracted from the total dose to give the measured dose, and the resulting measured to given dose ratio was 0.97 ± 0.03 for sample Rūdninkai 0.9 (XXVIII), and 0.96 ± 0.01 for sample Gaižiūnai 1.3 (XXIX), confirming that our feldspar $pIRIR_{290}$ measurement protocol is also able to measure accurately a dose given before any thermal pre-treatment.

Results

Grain-size distributions

The results of the grain-size analyses are presented in Table 2 and in Figures 3 and 4. Fine-grained sands dominate at all sites. The mean (Mz) values vary between 2.03 and 2.92 phi. Some parts of the Mikieriai profile contain coarser sand, with Mz values of 1.24 to 1.99 phi (at depths of 165 and 175 cm, respectively). The increase in coarser sand is also apparent at 1.5 m in the Mikieriai profile. The standard deviation (σ_1) varies from 0.37 to 1.45 and argues for the highest stability with time in the Gaižiūnai and Inkliuzai profiles; the latter is the best sorted. The coarser-grained part of the Mikieriai profile shows the poorest sorting. There is no clear trend in skewness (Sk); negative, positive, and symmetrical Sk with values ranging from −0.37 to 0.27 are found. Nevertheless, these sediments tend to have overall symmetrical characteristics.

Rounding and frosting

These sandy sediments are dominated by well-rounded (RM) and partially-rounded matt (EM/RM) grains (Table 3 and Figs. 3 and 4) in both fractions (0.5–0.8 and 0.8–1.0 mm) investigated here. The fraction of RM grains varies between 6% and 37% (both at the Rūdninkai 1 site) in the 0.5–0.8 mm fraction and between 3% (Mikieriai) and 44% (Rūdninkai 2a) in the 0.8–1.0 mm fraction; these values are considered as relatively high. The content of EM/RM grains varies between 11% (Inkliuzai) and 56% (Rūdninkai 1) in the 0.5–0.8 mm fraction, and between 9% (Mikieriai) and 65% (Rūdninkai 1) in the 0.8–1.0 mm fraction. The non-abraded weathered 'in situ' grains (NU/M) range from 0 to 20% and from 0 to 21% in the 0.5–0.8 mm and in the 0.8–1.0 mm fraction, respectively. The number of C type grains (resulting from breakage of EL, EM/EL, RM and EM/RM grains) is rather high and very variable with values between 3% (Rūdninkai 2) and 24% (Gaižiūnai) in the 0.5–0.8 mm fraction, and between 0% (Inkliuzai and Rūdninkai 2) and 30% (Gaižiūnai). The shiny grains, presumed to represent aquatic environments, make up 11% (EL grains), and up to 19% (EM/RM grains; both in the 0.8–1.0 mm fraction). In the 0.5–0.8 mm fraction, EL grains make up to 14%, while for EM/RM grains the percentage varies between 2 and 25%.

Mineral composition

The average quartz content in the 0.5–0.8 and in the 0.8–1.0 mm fractions is 69% and 60%, respectively. In general, the larger grain size fraction seems to contain less quartz; (between ~44% and ~74% in all profiles). All samples contain significant amounts of feldspar and particles of crystalline rocks (Table 4, Figs. 3 and 4); in the case of the lowermost parts of the Gaižiūnai and Inkliuzai profiles these two mineral groups make up >50% of the total mineral composition. There are very small amounts of micaceous minerals; these are only sporadically present in both size fractions, ranging between 0% and 3% in the Inkliuzai profile (Fig. 3).

Luminescence ages

A summary of the luminescence ages is presented in Table 1. With the exception of Inkliuzai 0,75 (XXV) (lab code 123095; quartz OSL age 41 ± 4 ka) the quartz ages range from 12.9 ± 1.0 ka (Mikieriai 2,1 (XXVI); lab code 123096) to 15.9 ± 1.0 ka (Gaižiūnai 1,3 (XXIX); lab code 123099). The $pIRIR_{290}$ ages derived from feldspar agree very well with these quartz ages (Table 1, Fig. 5), except for Inkliuzai 0,75 (XXV) (lab code 123095), for which the $pIRIR_{290}$ age is 181 ± 21 ka, more than four times older than the quartz age. This discrepancy is most likely explained by the differential bleaching rates of these quartz and feldspar luminescence signals (Buylaert et al., 2012; Murray et al., 2012): quartz is much easier to bleach in nature than feldspar; when quartz and

https://doi.org/10.1016/j.yqres.2015.04.001 Published online by Cambridge University Press

Table 2
Folk and Ward (1957) indicators of the investigated deposits: Mz = mean, σ = standard deviation, Sk = skewness.

Site		Depth [cm]	Mz	σ	Sk
Gaižiūnai		50	2.45	0.76	0.01
		60	2.25	0.76	0.13
		70	2.22	0.67	0.12
		80	2.11	0.70	0.20
		90	2.20	0.69	0.07
		100	2.24	0.62	0.12
		115	2.15	0.68	0.10
		130	2.33	0.62	0.00
		145	2.07	0.72	0.17
		150	2.28	0.64	0.06
		160	2.14	0.71	0.12
		170	2.17	0.68	0.11
		175	2.19	0.70	0.15
		185	2.03	0.73	0.17
		190	2.09	0.70	0.19
		200	2.11	0.69	0.14
		210	2.18	0.68	0.09
		230	2.26	0.66	0.01
		260	2.33	0.65	0.01
Inkluzai		40	2.80	0.42	0.12
		60	2.87	0.42	0.13
		70	2.76	0.54	−0.02
		80	2.92	0.44	0.19
		110	2.06	0.47	0.27
		120	1.99	0.55	0.14
		140	2.22	0.53	0.07
Mikierai		55	2.24	0.51	0.05
		65	2.23	0.48	0.13
		75	2.26	0.51	0.01
		80	2.29	0.51	−0.01
		95	2.10	0.57	0.10
		100	2.11	0.58	0.05
		105	2.22	0.56	0.03
		115	2.21	0.52	0.07
		120	2.14	0.57	0.05
		135	2.19	0.66	0.01
		140	2.03	0.67	0.08
		145	2.09	0.66	0.11
		155	1.98	0.72	0.14
		160	1.57	1.20	−0.13
		165	1.24	1.13	−0.19
		175	1.98	0.61	0.07
		190	2.36	0.55	−0.08
Rūdninkai	1	55	2.35	0.61	−0.18
		70	2.33	0.58	−0.17
		80	2.31	0.61	0.05
		85	2.37	0.69	−0.07
		100	2.38	0.69	−0.11
		110	2.43	0.55	−0.22
		120	2.42	0.56	−0.17
		130	2.43	0.57	−0.18
		140	2.43	0.55	−0.15
		150	2.36	0.56	−0.19
		165	2.24	0.67	−0.13
		175	1.82	1.03	−0.15
		180	1.94	0.90	−0.05
		185	2.22	0.65	−0.12
		210	2.21	0.66	−0.06
		250	2.16	0.72	−0.12
		280	2.20	0.74	−0.23
	2	35	2.30	0.54	−0.08
		60	1.83	0.77	0.09
		70	2.17	0.63	−0.01
		90	2.29	0.57	−0.11
		110	2.30	0.57	−0.13
		140	1.83	0.72	0.01
		150	1.80	0.74	0.21
	2a	60	2.25	0.73	−0.29
		90	2.32	0.62	−0.14
	3	60	2.30	0.66	−0.22
		80	2.29	0.63	−0.11
		90	2.32	0.61	−0.13

feldspar ages agree the luminescence signals in both minerals are almost certainly both well re-set prior to deposition (Murray et al., 2012). This applies to all our samples except Inkliuzai 0,75 (XXV) (laboratory ID 123095). Although a poorly-zeroed feldspar IRSL signal does not necessarily imply an overestimation for quartz, no further analyses were undertaken to test the degree of bleaching in this sample. In the next section we discuss the possible reliability of the quartz age using the sedimentary context.

Discussion

The proposed sedimentary–chronostratigraphic model of the Lithuanian inland eolian sediments allows us to consider the character of sediment transport and accumulation as well as the timing of eolian activity. In general, the stabilisation and subsequent re-activation phases of eolian accumulation is often controlled by high-frequency climate oscillations which are visible in e.g., the Greenland ice-core chronology (Svensson et al., 2008). Moreover, in Lithuania the process of sediment re-working is restricted to basins within e.g., glacial lakebeds, outwash fans or glaciofluvial terraces; there the dune fields seem to be compressed and nested (Guobytė and Satkūnas, 2011). In addition, eolian re-distribution only takes place when dry sand is available; this coincides with a change from relatively humid to relatively arid conditions (Swezey, 2001). Recent wind-tunnel experiments have revealed that in permafrost soils undergoing thawing–freezing cycles, the wind-driven sediment flux decreases with increasing soil moisture due to heavier particles and stronger inter-particle forces (Wang et al., 2014). Because of this, wind erosion is not important above a critical moisture content of 2.34% for frozen and of 2.61% for thawed soils (Wang et al., 2014). It seems likely that only the lowering of ground-water levels by drainage of ice-dammed lakes and sandurs, postglacial land uplift, and reduction of the permafrost table may trigger successful eolian activity (Zeeberg, 1998); these processes are strongly controlled by the position of the ice-margin. Nevertheless, under these circumstances formation of water table-influenced systems known as 'wet' eolian dune systems (Mountney, 2012) cannot be excluded. This is because of the presence of broad glaciofluvial plains and fluvial terraces, where the capillary fringe was in contact with the accumulation surface. This could have led to damp interdune elements interleaving laterally with architectural eolian dune elements (Mountney, 2012) as observed at Inkliuzai (cf. Fig. 2B). At Rūdninkai and Mikieriai the horizontal to low-angle lamination with the alternation of coarser and finer sands is subject to eolian sand-sheet deposition on the depositional surface which either alternated repeatedly from dry to wet conditions (Kasse, 2002 and references therein) or was influenced by changing wind velocities (Goździk, 1998). In conclusion, any reduction in wind velocity promotes deposition of wind-borne sediments; this explains the mixed nature of sediment sorting (Shrivastava et al., 2012). In contrast, high-angle tabular cross-stratification originates from saltation on dry surfaces. From this, we deduce that in our study area only the Gaižiūnai profile contains sediments representing a substantial dry-eolian sequence.

The overall characteristics and composition of the sediments are a function of source sediment composition, sediment transport, depositional processes, and weathering (Shrivastava et al., 2012) with transformation occurring in a particular (eolian) environment. The rounding and surface characteristics of quartz grains indicate a predominance of eolian mechanisms such as long-lasting abrasion and/or long transport distance (RM type of grains), and the short-lasting abrasion and/or short transportation (EM/RM type of grains) (Mycielska-Dowgiałło, 1993; Narayana et al., 2010; Ribolini et al., 2014). From laboratory experiments, Kuenen (1960) deduced that eolian abrasion is 100–1000× more effective than fluvial abrasion. In general, the presence of numerous well-rounded concavities taken together with surface frosting are likely to be a diagnostic indicator for eolian abrasion processes (Swezey, 1998), confirming the periglacial origin of the

Table 3
Rounding and frosting of quartz grains: NU/M — matt quartz grains with sharp edges, NU/L — shiny with sharp edges, EL — well-rounded shiny grains, RM — well-rounded matt grains, EM/EL — partially rounded shiny, EM/RM — partially rounded matt grains, C — cracked grains.

Site		Depth [cm]	0.5–0.8 mm							0.8–1.0 mm						
			NU/M	NU/L	EL	RM	EM/EL	EM/EM	C	NU/M	NU/L	EL	RM	EM/EL	EM/EM	C
Gaižiūnai		50	11	8	2	16	7	37	17	4	1	1	31	0.00	49	13
		60	9	9	2	29	10	32	8	–	–	–	–	–	–	–
		70	5	4	8	30	14	30	7	5	2	5	32	9	32	15
		80	9	6	7	24	16	19	19	14	0	2	28	8	44	3
		100	7	9	6	19	13	27	19	5	10	2	12	7	40	24
		115	5	13	4	16	19	19	23	6	10	5	17	8	39	15
		130	5	9	5	19	17	33	12	10	5	3	10	13	50	10
		145	2	6	8	30	13	26	16	14	7	2	16	13	32	16
		150	8	3	8	31	10	22	18	7	9	9	18	5	27	25
		170	3	6	6	21	14	28	23	3	8	3	19	6	28	35
		175	10	8	12	10	24	12	23	10	3	0	28	10	34	14
		190	9	8	14	22	25	16	6	3	3	8	18	5	45	20
		200	6	10	13	23	13	20	15	15	8	0	21	2	25	30
		210	3	8	6	19	25	16	24	–	–	–	–	–	–	–
		230	5	8	10	16	17	27	16	6	9	6	21	19	26	14
		260	5	11	13	15	24	13	18	7	0	7	9	9	52	18
Inkluzai		40	7	20	6	22	12	18	15	9	9	0	9	0	55	18
		60	11	17	1	29	7	28	6	21	5	0	16	5	42	11
		70	10	14	4	22	16	25	10	11	9	3	24	34	36	13
		80	12	2	2	36	6	32	10	–	–	–	–	–	–	–
		110	2	18	5	26	15	23	11	6	6	6	31	19	31	0
		120	6	20	7	28	18	11	11	8	22	2	27	8	15	18
		140	10	12	5	27	11	19	16	18	23	3	14	14	23	8
Mikierai		55	20	5	2	15	10	39	8	8	6	2	19	4	48	13
		65	2	26	6	8	19	25	13	7	7	3	3	17	41	21
		75	2	19	5	15	21	23	16	19	11	6	6	20	33	6
		80	9	9	4	20	11	28	20	–	–	–	–	–	–	–
		95	6	9	4	12	7	42	20	6	7	4	14	9	40	20
		100	5	11	8	10	17	34	16	7	15	1	21	18	28	10
		105	6	8	1	24	10	38	14	21	9	0	17	11	38	4
		120	6	12	5	11	18	36	12	8	11	11	11	11	36	11
		135	13	18	1	19	7	24	18	12	11	0	20	2	37	17
		145	10	3	1	20	12	38	17	8	3	2	24	5	52	6
		155	2	9	6	21	13	26	23	7	25	2	30	13	9	15
		160	5	7	3	21	7	47	11	7	8	3	28	2	39	14
		175	8	8	6	35	14	18	10	9	8	2	33	10	30	7
		190	4	24	3	20	11	15	22	0	7	3	23	19	32	17
Rūdninkai	1	55	4	1	1	30	11	46	7	2	0	0	38	2	49	9
		70	8	4	2	34	11	30	11	3	5	3	23	1	42	23
		80	5	6	2	22	11	40	14	3	1	0	23	5	60	8
		85	1	3	0	27	2	56	11	5	1	2	36	7	39	10
		100	4	7	3	34	2	34	16	5	1	0	38	6	44	6
		110	10	3	11	31	12	34	9	8	0	1	37	1	48	5
		120	6	14	8	16	17	33	6	2	1	0	36	10	44	7
		130	1	7	4	30	8	34	16	2	2	0	27	7	50	11
		140	3	11	8	24	21	29	3	2	2	0	12	4	58	20
		150	9	10	2	32	16	22	9	6	4	0	23	7	56	4
		165	4	4	3	23	15	37	15	6	2	1	29	2	41	17
		175	9	3	4	27	12	41	5	2	2	1	35	5	52	4
		180	1	6	5	29	10	30	18	2	2	1	25	1	49	19
		185	2	9	3	35	8	25	18	3	1	0	31	7	48	11
		210	2	9	6	22	10	29	22	6	10	4	28	9	30	14
		250	0	3	2	19	13	56	8	2	5	1	31	7	44	10
		280	5	3	2	25	8	42	15	2	2	1	22	5	65	4
	2	35	4	8	2	9	16	38	23	5	0	0	18	9	50	18
		60	8	8	1	27	4	35	16	5	10	0	23	7	40	15
		70	0	13	3	21	13	35	16	3	4	0	24	10	28	31
		90	2	5	6	21	4	36	26	1	1	0	25	5	43	25
		110	0	15	11	23	11	24	16	0	9	1	21	3	33	33
		140	2	7	3	14	9	30	34	2	5	1	24	2	45	20
		150	4	4	4	19	21	26	23	2	10	0	25	5	42	15
	2a	60	6	4	2	24	13	46	7	2	1	1	43	4	44	4
		90	4	4	2	21	13	45	12	3	2	3	27	3	48	14
	3	60	1	2	4	35	14	37	9	0	2	2	44	11	30	12
		80	1	8	7	15	11	38	18	0	12	0	26	1	22	28
		90	1	11	2	18	12	48	8	2	7	3	21	7	46	14

sediments (Zieliński et al., 2009). These features are unlikely to be inherited from former environments or be the product of dissolution (Werner and Merino, 1997). This is in contrast to the appearance of the remaining quartz grains found in our profiles, where either inheritance from former environments or chemical solution and re-deposition of silica has to be considered. Kuenen and Peredok (1962) have demonstrated experimentally that the latter can lead to rounding of quartz grains.

https://doi.org/10.1016/j.yqres.2015.04.001 Published online by Cambridge University Press

Table 4
Light minerals content: Q = quartz, F = feldspars, CR = particles of crystalline rocks.

Site		Depth [cm]	0.5–0.8 mm			0.8–1.0 mm		
			Q	F	CR	Q	F	CR
Gaižiūnai		50	78	20	2	68	26	7
		60	68	30	33	–	–	–
		70	71	24	6	54	39	8
		80	74	21	5	53	29	18
		100	73	20	6	61	26	13
		115	73	23	4	59	30	10
		130	64	24	11	63	27	10
		145	71	19	10	63	21	16
		150	72	22	6	59	35	5
		170	71	24	6	64	20	17
		175	73	21	6	65	26	9
		190	70	25	5	54	39	7
		200	76	21	3	67	21	10
		210	70	24	6	–	–	–
		230	76	17	6	45	36	18
		260	73	24	3	49	37	14
Inkluzai		40	69	25	4	44	30	26
		60	72	22	5	64	30	3
		70	67	29	4	60	23	17
		80	70	21	8	–	–	–
		110	69	25	6	57	43	0
		120	66	30	4	47	30	23
		140	60	33	7	55	27	26
Mikierai		55	49	45	7	53	35	12
		65	67	25	8	56	31	13
		75	68	23	9	56	29	16
		80	68	25	7	–	–	–
		95	67	29	4	58	30	13
		100	65	27	9	56	20	20
		105	60	32	7	49	41	10
		120	64	28	7	62	32	6
		135	77	20	3	49	38	13
		145	66	28	7	56	30	14
		155	60	33	7	61	28	11
		160	77	18	5	64	26	11
		175	78	18	4	61	25	14
		190	71	21	8	58	33	9
Rūdninkai	1	55	68	23	9	57	33	11
		70	76	15	10	70	20	11
		80	68	28	5	61	27	11
		85	69	30	1	59	31	10
		100	68	29	3	67	21	11
		110	63	33	4	63	27	10
		120	67	25	8	66	21	13
		130	77	20	4	62	32	6
		140	66	30	4	75	16	8
		150	76	23	1	65	27	8
		165	79	17	4	58	29	13
		175	69	29	2	59	32	8
		180	73	20	7	74	22	5
		185	72	23	4	67	26	7
		210	65	23	11	49	38	14
		250	73	25	3	59	32	9
		280	69	22	8	65	23	12
	2	35	71	23	6	70	30	0
		60	74	18	9	51	34	15
		70	75	20	5	65	23	13
		90	72	23	5	65	27	8
		110	64	24	12	62	25	13
		140	70	18	13	66	29	5
		150	72	17	10	71	21	9
	2a	60	68	27	5	56	36	8
		90	61	31	8	68	21	11
	3	60	63	30	7	64	16	21
		80	69	22	9	64	27	9
		90	58	36	6	64	22	14

Of the quartz grains of eolian origin, 10% show the textures typical of eolian transportation (Lisá, 2004). Shiny quartz grains have usually been subjected to fluvial or high-energy aqueous environments (Krinsley and Doornkamp, 1973; Sokołowski et al., 2014), and their abundance indicates a river floodplain or an estuarine shore face in a temperate climate (Marks et al., 2014). Severe abrasion as found in the intertidal zone or upper flow regimes is required to produce the subangular to rounded grain outline (Mahaney, 2002; Costa et al., 2012). A relatively high content of shiny and rounded/partially-rounded grains is rather unusual in eolian settings; however they have been observed within the eolian sand-sheets of central Poland (Kalińska, 2012) and in eolian complexes in Ukraine (Zieliński et al., 2009). The transportation/inheritance from neighbouring environments may explain the high content of fluvially transformed quartz grains in these sections.

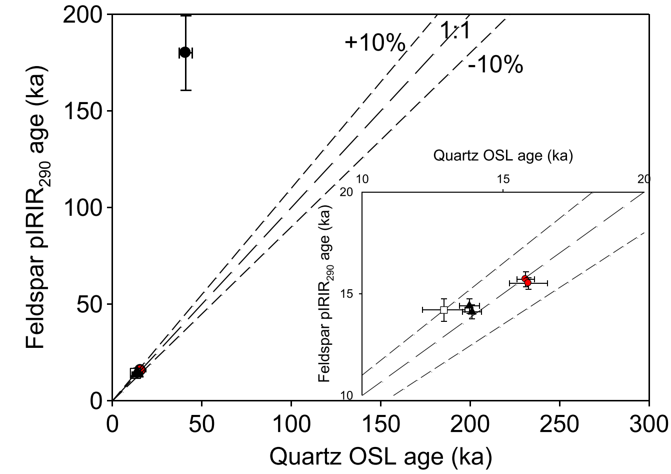

Figure 5. Comparison of quartz OSL and feldspar pIRIR$_{290}$ ages. The dashed line is the 1:1 line, and the medium dashed lines indicate ±10%. For all samples except one (lab code 123095; Inkliuzai 0,75 (XXV)) the ages are in good agreement and confirm sufficient signal re-setting for both quartz and feldspar. In the inset two distinct age clusters can be observed (within 1σ); these are referred to as older and younger eolian series. Red circles: Gaižiūnai; black triangle: Rūdninkai; white square: Mikieriai. Error bars represent random uncertainties only. See text for details.

Recent empirical studies (Langroudi et al., 2014) have revealed that quartz grain fracturing is not necessarily the result of energy input, nor a function of duration and grain size at the start of the process, but is more controlled by internal defects in quartz. However, it has been suggested that quartz grains with characteristic outlines reflecting their origin become fragmented due to cryogenic cracking, as a result of a combination of thermal shock, ice crystal growths in fissures, and hydration shattering (Schwamborn et al., 2012). These processes may in turn result from seasonal frost action (e.g., the open cracks in the surface of frozen ground are rapidly filled by sediment (Ribolini et al., 2014)) or transformation within the active layer (Woronko and Hoch, 2011; Woronko et al., 2013). However, at our sites there is no structural evidence for permafrost action. The ubiquitous presence of C-type quartz grains can thus be most easily explained as resulting from inheritance from the local glacial/glaciofluvial-bearing lithologies neighbouring the eolian deposits.

Petrographic data for sand grains, such as the relative proportions of quartz, feldspars, crystalline rocks, micaceous and other minerals provide information on the mineralogical maturity and may allow the identification of sediment source and provenance (Kasper-Zubillaga and Zolezzi-Ruiz, 2007; Tripaldi et al., 2010). A large proportion of mica or feldspar grains may preclude an eolian depositional environment (Swezey, 1998) because dune sands are usually considered to be multi-cyclic, being derived from multiply-recycled sediments (Howari et al., 2007). Given this, the significant occurrence of feldspars at all our Lithuanian localities is notable. This suggests that the major part of these sediments have not experienced multiple sedimentary cycles and their immature mineralogical composition indicates a nearby sediment source.

In summary, textural examination of these sediments revealed differences in their composition and origin. A number of proxies used in combination with the absolute OSL ages provide detailed insight into the eolian/glaciolacustrine–eolian record present in central and eastern Lithuania; the results enable us to identify distinct depositional series. Although no independent age control is as yet available to verify the accuracy of the luminescence ages, the agreement between quartz and feldspar ages (Fig. 5) can be interpreted as indicating complete bleaching of at least the quartz OSL prior to final deposition (Murray et al., 2012); incomplete bleaching is one of the most common causes of overestimation of age by OSL. In what follows, the sedimentary series are described based on their sedimentary features, from oldest to youngest.

The glaciolacustrine–eolian series

A quartz OSL age of 41 ± 4 ka was obtained at the Inkliuzai site; in contrast the feldspar age of the same sample was 181 ± 21 ka. This discrepancy may be explained by poor signal re-setting of the feldspar signal (see Results section), resulting in a significant age overestimate for feldspar. From our data it is not clear whether the quartz signal had been poorly reset prior to deposition.

The wavy–massive (*Sw*–*Sm*) structural alternation noted in the upper part of the Inkliuzai profile, and the higher mean/better sorting relationship (Fig. 3), might point to the occurrence of floodplain/shallow water conditions favourable for sediment settling from suspension. In contrast to the different mean/sorting values, however, the quartz rounding-frosting characteristics are rather similar to the other sites; no significant differences have been noted. This presence of micaceous minerals might point to settling in standing water, and the redeposition could be considered as a lacustrine–eolian sequence (Vandenberghe, 2013).

The older eolian series

Two sediment samples from the Gaižiūnai profile in the Central Lithuania provide self-consistent age of 15.9 ± 1.0 and 15.8 ± 0.9 ka and may possibly be correlated with the cold GS-2a event according to the GRIP stratigraphy (Björck et al., 1998; Walker et al., 1999). Indistinguishable ages of 15.7 ± 0.7 and 15.5 ± 0.7 ka were obtained from the feldspar extracts (Fig. 5), indicating that both minerals are likely to have been fully bleached. Rather cold and dry paleoenvironmental conditions favourable for eolian activity have been noted in NW Lithuania during the earliest stages of Lateglacial between 18,050 and 16,050 cal yr BP (Stančikaitė et al., 2008). This is reflected in the low organic productivity recorded in the sediments and the occurrence of pioneer, cold-tolerant species.

Typical eolian sedimentary architecture is manifested by the high-angle stratification of sands indicating the deposition on the distal slope of the dune (McKee, 1980; Zieliński and Issmer, 2008) and its successive migration and encroachment on older dunes (Zieliński et al., 2011). The eolian characteristics of these sediments seem to be less important further down in the sections (Fig. 3); similar proportions of fluvial- and eolian-type grains were noted in the lowermost part of the profile within the 0.5–0.8 mm fraction.

Turning to the textural record, the eolian sequence in the Gaižiūnai profile, with its decreasing fluvial/increasing eolian ratio of deposited sediments, is interestingly similar to some of the fluvial successions observed in NW Europe, indicating a regional increase towards aridity (Kasse, 1997, 2002; Kasse et al., 2007). However, that pattern is not supported by the larger (0.8–1.0 mm) grain-size fraction, where the grains are exposed to the strongest eolian abrasion in periglacial conditions (Mycielska-Dowgiałło and Dzierwa, 2003; Mycielska-Dowgiałło and Woronko, 2004). Combined with the deformations observed within the Gaižiūnai profile, some short-term and presumably local flood episodes (damp interdunes?) are reflected in the highest observed content of fluvially transformed quartz grains with simultaneous depletion of C (broken) grains. The latter is unlikely in water-dominated environments (cf. Marks et al., 2014).

The younger eolian series

For the eolian sediments exposed in Mikieriai and Rūdninkai our OSL ages range from 14.0 ± 0.8 ka to 12.0 ± 1.0 ka for quartz and 14.4 ± 0.7 ka to 14.1 ± 0.7 ka for feldspar. These ages coincide with a short period of climatic cooling known in the GRIP stratigraphy (Björck et al., 1998; Walker et al., 1999) as the GI-1d and 1c events, dated to between 14,050 and 13,150 cal yr BP. Within this younger eolian series, two subseries (older and younger) can be distinguished by comparison with stratigraphic interpretation, where the younger one (~12.0 ka based on quartz) at the Mikieriai site can be possibly attributed to the colder environmental conditions reflected in the calcareous gyttja layer. Diatom flora changes have been observed in southern Lithuania; these suggest water lowering under rather cold and oligotrophic conditions between ~13,200 and 12,600 cal yr BP (Šeirienė et al., 2009). Our luminescence ages cannot clearly distinguish between the two subseries (cf. Fig. 5) and so an unambiguous interpretation is not possible; a higher luminescence sampling frequency would be necessary to address this. The eolian sequence in Rūdninkai is mainly composed of climbing ripple cross-lamination (*Src*) representing deposition from saltation transport on dry ground at wind velocities between 4 and 8 m/s (Zieliński and Issmer, 2008). An accumulation in interdune areas, dune aprons, and sand sheets is support by the presence of low-angle stratification (Kocurek, 1986). The structureless sand observed in the part of the Mikieriai profile dated by OSL (Fig. 3) exemplifies both the sheet-like deposits (Bertran et al., 2011) and the almost total erasing of the original bedding structures by seasonal freezing and thawing (Kasse, 2002). The seasonal variations in wind velocity and wetness are reflected by the alternating bedding of finer- and coarser-grained sands (Kasse, 2002; Vandenberghe et al., 2013). The latter can be seen in some parts of the two Mikieriai profiles together with decreasing/increasing mean grain size values (Mz) and standard deviations (σ); the coarser-grained horizons show the poorest sorting (Figs. 3 and 4). The degree of grain rounding and frosting indicates that the eolian activity was greatest at the Rūdninkai 1 profile. The majority of grains are well- or partially rounded with matt surfaces (EM and EM/RM, respectively); they are undoubtedly the result from eolian transformation, either relatively long-lasting and/or active (RM type grains) and with short abrasion and transportation estimated at some hundreds of years (Mycielska-Dowgiałło, 1993). However, high-energy fluvial environment grains (EM/EL and EL) are also observed in the Rūdninkai and Mikieriai profiles and seem to increase within the upper part of profiles (Rūdninkai 1 and Mikieriai).

In southern Lithuanian paleolake environments, the beginning of gyttja deposition with a high number of *Slaginella selaginoides* L. and *Betula nana* L. has been noted for the time period 14,950–13,750 cal yr BP (Stančikaitė et al., 2008) together with an increasing number of heliophytes and *Armeria*, particularly in northwestern Lithuania. For northeastern Lithuania the paleobotanical record suggests scarcity of vegetation cover and a low content of organic matter in the sediments between 13,580 to 13,240 cal yr BP (Balakauskas et al., 2012). These paleobotanical records may be interpreted as indicative of the short-term climatic deterioration and may explain the decreasing number of eolian-type grains in the sediments.

Conclusions

A multi-proxy approach, combining various sedimentary–textural features together with luminescence dating has allowed a detailed depositional reconstruction of our study area. Eolian activity appears to be significantly older than expected from earlier research. Despite

https://doi.org/10.1016/j.yqres.2015.04.001 Published online by Cambridge University Press

the clear eolian conditions, the sediments show 'transitional' characteristics rather than pure eolian characteristics, possibly indicating that local glacial/glaciofluvial environments provided the main sediment source. Three clear phases of (glaciolacustrine–) eolian deposition are based on the optical ages. These are defined as follows: (1) A *glaciolacustrine–eolian phase* recorded in the Inkliuzai profile. The age of this material is not well defined; because of the large discrepancy between the quartz OSL age (41 ± 1 ka) and the feldspar $pIRIR_{290}$ age (181 ± 21 ka) we cannot be certain that the quartz was fully reset before burial. (2) An *older eolian phase* (~15–16 ka) at Gaižiūnai with typical eolian sedimentation reflecting successive migrating deposition on the distal slope of the dune. In addition, some short-term and presumably local flooding episodes were recorded. (3) The *younger eolian phases* in Rūdninkai and Mikieriai, dated to between 12.0 ± 1.0 and 14.0 ± 0.8 ka. The sedimentary features at Rūdninkai and Mikieriai suggest seasonal variations in wind velocity and wetness. Their formation was presumably controlled by the saltation transport succeeding in the deposition of interdune areas and sand sheets. The signs of eolian activity are the highest within eolian the series.

Even though the extent of ESB has not previously been thoroughly investigated; our sedimentary dataset together with luminescence ages allow a deeper understanding of the eolian mechanisms and environmental dynamics within the northeastern part of the ESB. The suitability of the material for luminescence dating opens up great opportunities for future work at higher resolution.

Acknowledgments

The authors wish to thank Tiit Rahe (Tallinn University of Technology) and Regina Morkūnaitė (Nature Research Centre, Vilnius) for their help during fieldwork. We are grateful to Albertas Bitinas for fruitful discussions. Prof. Vitālijs Zelčs (University of Latvia) is thanked for his support. We wish to thank Professor Andrei A. Velichko (Russian Academy of Sciences) and Dr. Jonas Satkūnas (Lithuanian Geological Survey) for their constructive reviews. The study was funded by the Postdoctoral Research Grant ERMOS (FP7 Marie Curie Cofund 'People' Programme) ERMOS22 (project reference: 246297) 'Age and climatic signature of coversands deposits distributed on glaciolacustrine basins along the Scandinavian Ice Sheet margin southeast of the Baltic Sea'.

References

Akulov, N.I., Rubtsova, M.N., 2011. Eolian deposits of rift zones. Quaternary International Elsevier Ltd and INQUA 234, 190–201. http://dx.doi.org/10.1016/j.quaint.2010.04.012 (http://linkinghub.elsevier.com/retrieve/pii/S1040618210001357).

Balakauskas, L., Taminskas, J., Mazeika, J., Stancikaite, M., 2012. Lateglacial and early-Holocene palaeohydrological changes in the upper reaches of the Ula River: an example from southeastern Lithuania. The Holocene 23, 117–126. http://dx.doi.org/10.1177/0959683612455552 (http://hol.sagepub.com/cgi/doi/10.1177/0959683612455552).

Bateman, M.D., Van Huissteden, J., 1999. The timing of last-glacial periglacial and eolian events, Twente, eastern Netherlands. J. Quat. Sci. 14, 277–283.

Bertran, P., Bateman, M.D., Hernandez, M., Mercier, N., Millet, D., Sitzia, L., Tastet, J.-P., 2011. Inland eolian deposits of south-west France: facies, stratigraphy and chronology. J. Quat. Sci. 26, 374–388. http://dx.doi.org/10.1002/jqs.1461 (http://doi.wiley.com/10.1002/jqs.1461).

Bitinas, A., 2004. The age of eolian deposits in Lithuania. Geologija 45, 1–5.

Bitinas, A., Damušytė, A., Stančikaitė, M., Aleksa, P., 2002. Geological development of the Nemunas River Delta and adjacent areas, West Lithuania. Geol. Quart. 46, 375–389.

Björck, S., Walker, M.J.C., Cwynar, L.C., Johnsen, S., Knudsen, K.-L., Lowe, J.J., Wohlfarth, B., 1998. An event stratigraphy for the Last Termination in the North Atlantic region based on the Greenland ice-core record: a proposal by the INTIMATE group. J. Quat. Sci. 13, 283–292 (http://doi.wiley.com/10.1002/%28SICI%291099-1417%28199807/08%2913%3A4%3C283%3A%3AAID-JQS386%3E3.0.CO%3B2-A, http://dx.doi.org/10.1002/(SICI)1099-1417(199807/08)13:4283::AID-JQS386/;3.0.CO;2-A).

Blažauskas, N., Jurgaitis, A., Šinkūnas, P., 1998. Sedimentation of Quaternary sandy deposits in South Lithuania. Litosfera 2, 87–100.

Blažauskas, N., Jurgaitis, A., Šinkūnas, P., 2007. Patterns of Late Pleistocene proglacial fluvial sedimentation in the SE Lithuanian Plain. Sediment. Geol. 193, 193–201. http://dx.doi.org/10.1016/j.sedgeo.2005.06.015 (http://linkinghub.elsevier.com/retrieve/pii/S0037073806002582).

Buylaert, J.-P., Jain, M., Murray, A.S., Thomsen, K.J., Thiel, C., Sohbati, R., 2012. A robust feldspar luminescence dating method for Middle and Late Pleistocene sediments. Boreas 41, 435–451. http://dx.doi.org/10.1111/j.1502-3885.2012.00248.x (http://doi.wiley.com/10.1111/j.1502-3885.2012.00248.x).

Cailleux, A., 1942. Les actiones éoliennes périglaciaires en Europe. Mém. Soc. Géol. Fr. 41, 1–176.

Costa, P.J.M., Andrade, C., Dawson, a.G., Mahaney, W.C., Freitas, M.C., Paris, R., Taborda, R., 2012. Microtextural characteristics of quartz grains transported and deposited by tsunamis and storms. Sediment. Geol. 275–276, 55–69. http://dx.doi.org/10.1016/j.sedgeo.2012.07.013 (http://linkinghub.elsevier.com/retrieve/pii/S0037073812002035).

Darrénougué, N., De Deckker, P., Fitzsimmons, K.E., Norman, M.D., Reed, L., van der Kaars, S., Fallon, S., 2009. A late Pleistocene record of eolian sedimentation in Blanche Cave, Naracoorte, South Australia. Quat. Sci. Rev. 28, 2600–2615. http://dx.doi.org/10.1016/j.quascirev.2009.05.021 (http://linkinghub.elsevier.com/retrieve/pii/S0277379109001875).

Duller, G.A.T., 2003. Distinguishing quartz and feldspar in single grain luminescence measurements. Radiat. Meas. 37, 161–165. http://dx.doi.org/10.1016/S1350-4487(02)00170-1 (http://linkinghub.elsevier.com/retrieve/pii/S1350448702001701).

Folk, R.L., Ward, W.C., 1957. Brazos River bar: a study in the significance of grain size parameters. J. Sediment. Petrol. 27, 3–26.

Gaigalas, A., Pazdur, A., 2008. Chronology of buried soils, forest fires and extreme migration of dunes on the Kuršių nerija spit (Lithuanian coast). Landf. Anal. 9, 187–191.

Gilbert, E.R., De Camargo, M.G., Sandrini-Neto, L., 2012. Rysgran: Grain Size Analysis, Textural Classifications and Distribution of Unconsolidated Sediments.

Goździk, J., 1998. Struktury sedymentacyjne w eolicznych piaskach pokrywowych w Polsce. In: Mycielska-Dowgiałło, E. (Ed.), Struktury sedymentacyjne i postsedymentacyjne w osadach czwartorzędowych i ich wartość interpretacyjna. Uniwersytet Warszawski, Warsaw, pp. 167–191.

Gudelis, V., 1998. A catastrophic dune forest fire on the Kuršiu Nerija spit (Lithuanian coast) and its impact on the coastal population in Late Neolithic times. Pact 54, 45–50.

Gudelis, V., Michaliukaitė, E., 1976. Ancient parabolic dunes on the spit of Kuršių Nerija. Geogr. Lith. V 56–63.

Guobytė, R., Satkūnas, J., 2011. Chapter 19 — Pleistocene glaciations in Lithuania. Dev. Quat. Sci. 15, 231–246. http://dx.doi.org/10.1016/B978-0-444-53447-7.00019-2 (http://www.sciencedirect.com/science/article/pii/B9780444534477000192).

Howari, F.M., Baghdady, A., Goodell, P.C., 2007. Mineralogical and gemorphological characterization of sand dunes in the eastern part of United Arab Emirates using orbital remote sensing integrated with field investigations. Geomorphology 83, 67–81. http://dx.doi.org/10.1016/j.geomorph.2006.06.015 (http://linkinghub.elsevier.com/retrieve/pii/S0169555X06002431).

Huntley, D.J., Baril, M.R., 1997. The K content of the K-feldspars being measured in optical dating or in thermoluminescence dating. Ancient TL 15, 11–13.

Huntley, D.J., Hancock, R.G.V., 2001. The Rb contents of K-feldspar grains being measured in optical dating. Ancient TL 19, 43–46.

Jankowski, M., 2012. Lateglacial soil paleocatena in inland-dune area of the Toruń Basin, Northern Poland. Quat. Int. 265, 116–125. http://dx.doi.org/10.1016/j.quaint.2012.02.006 (http://linkinghub.elsevier.com/retrieve/pii/S1040618212000730).

Kaiser, K., Hilgers, A., Schlaak, N., Jankowski, M., Kühn, P., Bussemer, S., Przegiętka, K., 2009. Palaeopedological marker horizons in northern central Europe: characteristics of Lateglacial Usselo and Finow soils. Boreas 38, 591–609. http://dx.doi.org/10.1111/j.1502-3885.2008.00076.x (http://doi.wiley.com/10.1111/j.1502-3885.2008.00076.x).

Kalińska, E., 2012. Geological setting and sedimentary characteristics of the coversands distributed in the western part of the Blonie glaciolacustrine basin (Central Poland) — preliminary results. Bull. Geol. Soc. Finl. 84, 33–44.

Kalińska, E., Nartišs, M., 2014. Pleistocene and Holocene eolian sediments of different location and geological history: a new insight from rounding and frosting of quartz grains. Quat. Int. 328–329, 311–322. http://dx.doi.org/10.1016/j.quaint.2013.08.038.

Kalińska-Nartiša, E., Nartišs, M., Thiel, C., Buylaert, J.-P., Murray, A.S., 2014. Late-glacial to Holocene eolian deposition in northeastern Europe — the timing of sedimentation at the Iisaku site (NE Estonia). Quat. Int. http://dx.doi.org/10.1016/j.quaint.2014.08.039.

Kasper-Zubillaga, J.J., Zolezzi-Ruiz, H., 2007. Grain size, mineralogical and geochemical studies of coastal and inland dune sands from El Vizcaíno Desert, Baja California Peninsula, Mexico. Rev. Mex. Cienc. Geol. 24, 423–438.

Kasse, C., 1997. Cold-climate eolian sand-sheet formation in North-Western Europe (c. 14–12.4 ka); a response to permafrost degradation and increased aridity. Permafr. Periglac. Process. 8, 295–311.

Kasse, C., 2002. Sandy eolian deposits and environments and their relation to climate during the Last Glacial Maximum and Lateglacial in northwest and central Europe. Prog. Phys. Geogr. 26, 507–532. http://dx.doi.org/10.1191/0309133302pp350ra (http://ppg.sagepub.com/cgi/doi/10.1191/0309133302pp350ra).

Kasse, C., Vandenberghe, D., De Corte, F., Van Den Haute, P., 2007. Late Weichselian fluvio-eolian sands and coversands of the type locality Grubbenvorst (southern Netherlands): sedimentary environments, climate record and age. J. Quat. Sci. 22, 695–708. http://dx.doi.org/10.1002/jqs.

Kocurek, G., 1986. Origins of low-angle stratification in eolian deposits. Eolian geomorphology. Proceedings of the 17th Annual Inghampton Geomorphology Symposium. Allen & Unwin, London, pp. 177–195.

Kolstrup, E., 2007. Lateglacial older and younger coversand in northwest Europe: chronology and relation to climate and vegetation. Boreas 36, 65–75. http://dx.doi.org/10.1080/03009480600827280 (http://doi.wiley.com/10.1080/03009480600827280).

Koster, E.A., 2005. Recent advances in luminescence dating of Late Pleistocene (cold-climate) eolian sand and loess deposits in western Europe. Permafr. Periglac. Process. 16, 131–143. http://dx.doi.org/10.1002/ppp.512 (http://doi.wiley.com/10.1002/ppp.512).

Koster, E.A., 2009. The "European Eolian Sand Belt": Geoconservation of Drift Sand Landscapes. pp. 93–110 http://dx.doi.org/10.1007/s12371-009-0007-8.

Krinsley, D.H., Doornkamp, J.C., 1973. Atlas of Quartz Sand Surface Textures. Cambridge University Press, Oxford, pp. 1–93.

Kuenen, P.H., 1960. Experimental abrasion 4: eolian action. J. Geol. 4, 427–449.

Kuenen, P.H., Peredok, W.G., 1962. Experimental abrasion 5. Frosting and defrosting of quartz grains. J. Geol. 70, 648–658.

Küster, M., Fülling, A., Kaiser, K., Ulrich, J., 2014. Eolian sands and buried soils in the Mecklenburg Lake District, NE Germany: Holocene land-use history and pedo-geomorphic response. Geomorph. Elsevier B.V. 211, 64–76. http://dx.doi.org/10.1016/j.geomorph.2013.12.030 (http://linkinghub.elsevier.com/retrieve/pii/S0169555X13006387).

Langroudi, A., A., Jefferson, I., O'hara-Dhand, K., Smalley, I., 2014. Geomorphology micromechanics of quartz sand breakage in a fractal context. 211 pp. 1–10.

Lisá, L., 2004. Exoscopy of Moravian eolian sediments. Bull. Geosci. 79, 177–182.

Mahaney, W.C., 2002. Atlas of Sand Grain Surface, Textures and Applications. Oxford University Press, Oxford.

Marks, L., Gałązka, D., Krzymińska, J., Nita, M., Stachowicz-Rybka, R., Witkowski, A., Woronko, B., Dobosz, S., 2014. Marine transgressions during Eemian in northern Poland: a high resolution record from the type section at Cierpięta. Quat. Int. 328–329, 45–59. http://dx.doi.org/10.1016/j.quaint.2013.12.007 (http://linkinghub.elsevier.com/retrieve/pii/S1040618213009270).

McKee, E.K., 1980. A study of global sand seas: introduction to a study of global sand seas. US Geological Survey, Professional Paper (450 pp).

Mejdahl, V., 1979. Thermoluminescence dating: beta-dose attenuation in quartz grains. Archaeometry 21, 61–72.

Miall, A.D., 1977. Lithofacies types and vertical profile models in braided river deposits: a summary. Fluvial Sedimentol. 5, 597–604.

Miall, A.D., 1978. Lithofacies types and vertical profile models in braided river deposits: a summary. In: Miall, A.D. (Ed.), Fluvial Sedimentology. Can. Soc. Petrol. Geol. Mem., pp. 597–604.

Molodkov, A., Bitinas, A., 2006. Sedimentary record and luminescence chronology of the Lateglacial and Holocene eolian sediments in Lithuania. Boreas 35, 244–254. http://dx.doi.org/10.1080/03009480600584915.

Mountney, N.P., 2012. A stratigraphic model to account for complexity in eolian dune and interdune successions. Sedimentology 59, 964–989. http://dx.doi.org/10.1111/j.1365-3091.2011.01287.x (http://doi.wiley.com/10.1111/j.1365-3091.2011.01287.x).

Muhs, D.R., 2004. Mineralogical maturity in dunefields of North America, Africa and Australia. Geomorphology 59, 247–269. http://dx.doi.org/10.1016/j.geomorph.2003.07.020 (http://linkinghub.elsevier.com/retrieve/pii/S0169555X03003271).

Murray, A.S., Wintle, A.G., 2000. Luminescence dating of quartz using an improved single-aliquot regenerative-dose protocol. Radiat. Meas. 32, 57–73. http://dx.doi.org/10.1016/S1350-4487(99)00253-X (http://linkinghub.elsevier.com/retrieve/pii/S135044879900253X).

Murray, A.S., Marten, R., Johnston, A., Martin, P., 1987. Analysis for naturally occuring radionuclides at environmental concentrations by gamma spectrometry. J. Radioanal. Nucl. Chem. 115, 263–288.

Murray, A.S., Thomsen, K.J., Masuda, N., Buylaert, J.P., Jain, M., 2012. Identifying well-bleached quartz using the different bleaching rates of quartz and feldspar luminescence signals. Radiat. Meas. 47, 688–695.

Mycielska-Dowgiałło, E., 1993. Estimates of Late Glacial and Holocene eolian activity in Belgium, Poland and Sweden. Boreas 22, 165–170. http://dx.doi.org/10.1111/j.1502-3885.1993.tb00177.x.

Mycielska-Dowgiałło, E., 2007. Metody badań cech teksturalnych osadów klastycznych i wartość interpretacyjna wyników. In: Mycielska-Dowgiałło, Elżbieta, Rutkowski, J. (Eds.), Badania cech teksturalnych osadów czwartorzędowych i wybrane metody oznaczania ich wieku. WSWPR, pp. 95–189.

Mycielska-Dowgiałło, E., Dzierwa, K., 2003. Rekonstrucja dynamiki procesów eolicznych i czasu ich trwania na podstawie wybranych cech teksturalnych osadów wydmy w Cięciwie. Prz. Geol. 51, 163–167.

Mycielska-Dowgiałło, E., Woronko, B., 1998. Analiza obtoczenia i zmatowienia powierzchni ziarn kwarcowych frakcji piaszczystej i jej wartość interpretacyjna. Prz. Geol. 46, 1275–1281.

Mycielska-Dowgiałło, E., Woronko, B., 2004. The degree of aeolization of Quaternary deposits in Poland as a tool for stratigraphic interpretation. Sediment. Geol. 168, 149–163. http://dx.doi.org/10.1016/j.sedgeo.2003.12.006 (http://linkinghub.elsevier.com/retrieve/pii/S0037073803003737).

Narayana, A.C., Mohan, R., Mishra, R., 2010. Morphology and surface textures of quartz grains from freshwater lakes of McLeod Island, Larsemann Hills, East Antarctica. Curr. Sci. 99, 1420–1424.

Olley, J.M., Murray, A.S., Roberts, R.G., 1996. The effects of disequilibria in the uranium and thorium decay chains on burial dose rates in fluvial sediments. Quat. Sci. Rev. 15, 751–760.

Prescott, J.R., Hutton, J.T., 1994. Cosmic ray contributions to dose rates for luminescence and ESR dating: large depths and long-term time variations. Radiat. Meas. 23, 497–500.

Ribolini, A., Bini, M., Consoloni, I., Isola, I., Pappalardo, M., Zanchetta, G., Fucks, E., Panzeri, L., Martini, M., Terrasi, F., 2014. Late-Pleistocene wedge structures along the Patagonian Coast (Argentina): chronological constraints and palaeo-environmental implications. Geogr. Ann. A Phys. Geogr. http://dx.doi.org/10.1111/geoa.12038 (http://doi.wiley.com/10.1111/geoa.12038).

Rinterknecht, V.R., Clark, P.U., Raisbeck, G.M., Yiou, F., Bitinas, A., Brook, E.J., Marks, L., Zelcs, V., Lunkka, J.-P., Pavlovskaya, I.E., Piotrowski, J.A., Raukas, A., 2006. The last deglaciation of the southeastern sector of the Scandinavian ice sheet. Science (New York, N.Y.) 311, 1449–1452. http://dx.doi.org/10.1126/science.1120702 (http://www.ncbi.nlm.nih.gov/pubmed/16527977).

Rinterknecht, V.R., Bitinas, A., Clark, P.U., Raisbeck, G.M., Yiou, F., Brook, E.J., 2008. Timing of the last deglaciation in Lithuania. Boreas 37, 426–433. http://dx.doi.org/10.1111/j.1502-3885.2008.00027.x (http://doi.wiley.com/10.1111/j.1502-3885.2008.00027.x).

Satkūnas, J., 1993. Conditions of Occurrence, Structure and Forming Peculiarities of the Interglacial Sediments in Eastern Lithuania. Vilnius (26 pp).

Satkūnas, J.A., Gaigalas, A.I., Hütt, G.I., 1991. Lithogenesis and formation time of the Skersabaliai eolian massif. Geokronologicheskie i izotopno-geokhimicheskie issledovaniya v chetviertnichnoj geologii i arkheologii. Vilnius University Press, Vilnius, pp. 14–26.

Satkūnas, J., Grigiene, A., Jusiene, A., Damusyte, A., Mazeika, J., 2009. Middle Weichselian palaeolacustrine basin in the Venta river valley and vicinity (northwest Lithuania), exemplified by the Purviai outcrop. Quaternary International Elsevier Ltd and INQUA 207, 14–25. http://dx.doi.org/10.1016/j.quaint.2008.12.003 (http://linkinghub.elsevier.com/retrieve/pii/S1040618208003509).

Schwamborn, G., Schirrmeister, L., Frütsch, F., Diekmann, B., 2012. Quartz weathering in freeze–thaw cycles: experiment and application to the El'Gygytgyn crater lake record for tracing Siberian permafrost history. Geogr. Ann. A Phys. Geogr. 94, 481–499. http://dx.doi.org/10.1111/j.1468-0459.2012.00472.x (http://doi.wiley.com/10.1111/j.1468-0459.2012.00472.x).

Šeirienė, V., Kabailienė, M., Kasperovičienė, J., Mažeika, J., Petrošius, R., Paškauskas, R., 2009. Reconstruction of postglacial palaeoenvironmental changes in eastern Lithuania: evidence from lacustrine sediment data. Quat. Int. 207, 58–68. http://dx.doi.org/10.1016/j.quaint.2008.12.005.

Shrivastava, P.K., Asthana, R., Roy, S.K., Swain, A.K., Dharwadkar, A., 2012. Provenance and depositional environment of epi-shelf lake sediment from Schirmacher Oasis, East Antarctica, vis-à-vis scanning electron microscopy of quartz grain, size distribution and chemical parameters. Polar Sci. 6, 165–182. http://dx.doi.org/10.1016/j.polar.2012.03.006 (http://linkinghub.elsevier.com/retrieve/pii/S1873965212000126).

Sokołowski, T., Wacnik, A., Woronko, B., Madeja, J., 2014. Eemian Weichselian pleniglacial fluvial deposits in S Poland (an example of the Vistula River valley in Kraków). Geol. Quart. 58, 71–84. http://dx.doi.org/10.7306/gq.1138 (https://gq.pgi.gov.pl/article/view/9273).

Stančikaitė, M., 2006. Late glacial environmental history in Lithuania. Archaeol. Balt. 7, 199–208.

Stančikaitė, M., Kisielienė, D., Strimaitienė, A., 2004. Vegetation response to the climatic and human impact changes during the Late Glacial and Holocene: case study of the marginal area of Baltija Upland, NE Lithuania. Baltica 17, 17–33.

Stančikaitė, M., Šinkūnas, P., Šeirienė, V., Kisielienė, D., 2008. Patterns and chronology of the Lateglacial environmental development at Pamerkiai and Kašušiai, Lithuania. Quat. Sci. Rev. 27, 127–147. http://dx.doi.org/10.1016/j.quascirev.2007.01.014.

Stančikaitė, M., Kisielienė, D., Moe, D., Vaikutienė, G., 2009. Lateglacial and early Holocene environmental changes in northeastern Lithuania. Quat. Int. 207, 80–92. http://dx.doi.org/10.1016/j.quaint.2008.10.009.

Svensson, A., Andersen, K.K., Bigler, M., Clausen, H.B., Dahl-Jensen, D., Davies, S.M., Johnsen, S.J., Muscheler, R., Parrenin, F., Rasmussen, S.O., Röthlisberger, R., Seierstad, I., Steffensen, J.P., Vinther, B.M., 2008. A 60000 year Greenland stratigraphic ice core chronology. Clim. Past 4, 47–57. http://dx.doi.org/10.5194/cp-4-47-2008 (http://www.clim-past.net/4/47/2008/).

Swezey, C.S., 1998. The indentification of eolian sands and sandstones. C. R. Acad. Sci. 327, 513–518.

Swezey, C.S., 2001. Sequence stratigraphy in eolian systems. AAPG Annual Convention Program, p. A196.

Thiel, C., Buylaert, J.-P., Murray, A., Terhorst, B., Hofer, I., Tsukamoto, S., Frechen, M., 2011. Luminescence dating of the Stratzing loess profile (Austria) — testing the potential of an elevated temperature post-IR IRSL protocol. Quaternary International Elsevier Ltd and INQUA 234, 23–31. http://dx.doi.org/10.1016/j.quaint.2010.05.018 (http://linkinghub.elsevier.com/retrieve/pii/S1040618210002156).

Tolksdorf, J.F., Kaiser, K., 2012. Holocene eolian dynamics in the European sand-belt as indicated by geochronological data. Boreas 41, 408–421. http://dx.doi.org/10.1111/j.1502-3885.2012.00247.x (http://doi.wiley.com/10.1111/j.1502-3885.2012.00247.x).

Tripaldi, A., Ciccioli, P.L., Alonso, M.S., Forman, S.L., 2010. Petrography and geochemistry of late Quaternary dune fields of western Argentina: Provenance of eolian materials in southern South America. Eolian Res. Elsevier B.V. 2, 33–48. http://dx.doi.org/10.1016/j.aeolia.2010.01.001 (http://linkinghub.elsevier.com/retrieve/pii/S1875963710000029).

Van der Hammen, T., 1951. Late-glacial flora and periglacial phenomena in the Netherlands. Leidse. Geol. Meded. 17, 71–183.

Van der Hammen, T., Wijmstra, T.A., 1971. The Upper Quaternary of the Dinkel valley (Twente, Eastern Overijssel, the Netherlands). Med. Rijsk Geol. Dienst 22, 55–212.

Vandenberghe, J., 2013. Grain size of fine-grained windblown sediment: a powerful proxy for process identification. Earth Sci. Rev. 121, 18–30. http://dx.doi.org/10.1016/j.earscirev.2013.03.001 (http://linkinghub.elsevier.com/retrieve/pii/S0012825213000469).

Vandenberghe, D.A.G., Derese, C., Kasse, C., Van den Haute, P., 2013. Late Weichselian (fluvio-)eolian sediments and Holocene drift-sands of the classic type locality in Twente (E Netherlands): a high-resolution dating study using optically stimulated luminescence. Quat. Sci. Rev. Elsevier Ltd 68, 96–113. http://dx.doi.org/10.1016/j.quascirev.2013.02.009 (http://linkinghub.elsevier.com/retrieve/pii/S0277379113000632).

Velichko, A.A., Catto, N.R., Yu Kononov, M., Morozova, T.D., Yu Novenko, E., Panin, P.G., Ya Ryskov, G., Semenov, V.V., Timireva, S.N., Titov, V.V., Tesakov, A.S., 2009. Progressively cooler, drier interglacials in southern Russia through the Quaternary: evidence from the Sea of Azov region. Quat. Int. 198, 204–219. http://dx.doi.org/10.1016/j.quaint.2008.06.005 http://linkinghub.elsevier.com/retrieve/pii/S1040618208001912.

Vieira, G.T., Mycielska-Dowgiallo, E., Woronko, B., 2003. Sedimentological analysis of sandy-gravel accumulations, Serra da Estrela plateaux (Portugal). Landf. Anal. 4, 99–107.

Walker, M.J.C., Bjo, S., Lowe, J.J., Cwynar, L.C., Johnsen, S., Knudsen, K., Wohlfarth, B., 1999. Isotopic “events” in the GRIP ice core: a stratotype for the Late Pleistocene. Quat. Sci. Rev. 18, 1143–1150.

Wang, L., Shi, Z.H., Wu, G.L., Fang, N.F., 2014. Freeze/thaw and soil moisture effects on wind erosion. Geomorphology 207, 141–148.

Werner, B.T., Merino, E., 1997. Concave sand grains in eolian envrionemnts: evidence, mechanism, and modeling. J. Sediment. Res. 67, 754–762.
Wintle, A.G., 2008. Luminescence dating: where it has been and where it is going. Boreas 37, 471–482. http://dx.doi.org/10.1111/j.1502-3885.2008.00059.x http://doi.wiley.com/10.1111/j.1502-3885.2008.00059.x.
Wintle, A.G., Murray, A.S., 2006. A review of quartz optically stimulated luminescence characteristics and their relevance in single-aliquot regeneration dating protocols. Radiat. Meas. 41, 369–391. http://dx.doi.org/10.1016/j.radmeas.2005.11.001 http://linkinghub.elsevier.com/retrieve/pii/S1350448705003227.
Woronko, B., 2012. Micromorphology of quartz grains as a tool in the reconstruction of periglacial environment. In: Churski, P. (Ed.), Contemporary Issues in Polish, Geography, pp. 111–131.
Woronko, B., Hoch, M., 2011. The development of frost-weathering microstructures on sand-sized quartz grains: examples from Poland and Mongolia. Permafr. Periglac. Process. 227, 214–227. http://dx.doi.org/10.1002/ppp.725 http://doi.wiley.com/10.1002/ppp.725.
Woronko, B., Rychel, J., Karasiewicz, M.T., Ber, A., Krzywicki, T., Marks, L., Pochocka-Szwarc, K., 2013. Heavy and light minerals as a tool for reconstructing depositional environments: an example from the Jałówka site (northern Podlasie region, NE Poland). Geologos 19, 47–66. http://dx.doi.org/10.2478/logos-2013-0004 http://www.degruyter.com/view/j/logos.2013.19.issue-1-2/logos-2013-0004/logos-2013-0004.xml.
Zeeberg, J., 1998. The European sand belt in eastern Europe — and comparison of Late Glacial dune orientation with GCM simulation results. Boreas 27, 127–139.
Zieliński, P., Issmer, K., 2008. Propozycja kodu genetycznego osadów środowiska eolicznego. Prz. Geol. 56, 67–72.
Zieliński, P., Fedorowicz, S., Zaleski, I., 2009. Sedimentary succession in Berezno in the Volhynia Polesie (Ukraine) as an example of depositional environment changes in the periglacial zone at the turn of the Vistulian and the Holocene. Geologija 51, 97–108. http://dx.doi.org/10.2478/v10056-009-0011-3 http://versita.metapress.com/openurl.asp?genre=article&id=doi:10.2478/v10056-009-0011-3.
Zieliński, P., Sokołowski, R.J., Fedorowicz, S., Jankowski, M., 2011. Stratigraphic position of fluvial and eolian deposits in the Żabinko site (W Poland) based on TL dating. Geochronometria 38. http://dx.doi.org/10.2478/s13386-011-0005-x http://www.springerlink.com/index/10.2478/s13386-011-0005-x.